

## Article

# Development of an Experimental Dead-End Microfiltration Layout and Process Repeatability Analysis

Gorazd Bombek <sup>1,\*</sup>, Luka Kevorkijan <sup>1</sup>, Grega Hrovat <sup>2</sup>, Drago Kuzman <sup>2</sup>, Aleks Kapun <sup>2</sup>, Jure Ravnik <sup>1</sup> , Matjaž Hriberšek <sup>1</sup> and Aleš Hribernik <sup>1</sup> 

<sup>1</sup> Faculty of Mechanical Engineering, University of Maribor, 2000 Maribor, Slovenia; luka.kevorkijan@um.si (L.K.); jure.ravnik@um.si (J.R.); matjaz.hribersek@um.si (M.H.); ales.hribernik@um.si (A.H.)

<sup>2</sup> Novartis Pharma, 1234 Mengeš, Slovenia; grega-1.hrovat@novartis.com (G.H.); drago.kuzman@novartis.com (D.K.); aleks.kapun@novartis.com (A.K.)

\* Correspondence: gorazd.bombek@um.si; Tel.: +386-22207739

**Abstract:** Microfiltration is an important process in the pharmaceutical industry. Filter selection and validation is a time-consuming and expensive process. Quality by design approach is important for product safety. The article covers the instrumentalization and process control of a laboratory-scale dead-end microfiltration layout. The layout is a downscale model of the actual production line, and the goal is filter validation and analysis of process parameters, which may influence filter operation. Filter size, fluid pressure, valve plunger speed, and timing issues were considered. The focus is on the identification of the most influential process parameters and their influence on the repeatability of pressure oscillations caused by valve opening. The goal was to find the worst-case scenario regarding pressure oscillations and, consequently, filter energy intake. The layout was designed as compact as possible to reduce pressure losses between the filter and valve. Valve-induced pressure oscillations proved to be prevailing over the water hammer effect. Several filters in sizes between 3.5 cm<sup>2</sup> and 6900 cm<sup>2</sup> were tested, and some recommendations were suggested for the reduction of energy intake of the filter and to improve the repeatability of the process.

**Keywords:** filtration; pressure oscillations; repeatability; process; parameter



**Citation:** Bombek, G.; Kevorkijan, L.; Hrovat, G.; Kuzman, D.; Kapun, A.; Ravnik, J.; Hriberšek, M.; Hribernik, A. Development of an Experimental Dead-End Microfiltration Layout and Process Repeatability Analysis. *Processes* **2024**, *12*, 253. <https://doi.org/10.3390/pr12020253>

Academic Editor: Roberto Pisano

Received: 19 December 2023

Revised: 16 January 2024

Accepted: 18 January 2024

Published: 24 January 2024



**Copyright:** © 2024 by the authors. Licensee MDPI, Basel, Switzerland. This article is an open access article distributed under the terms and conditions of the Creative Commons Attribution (CC BY) license (<https://creativecommons.org/licenses/by/4.0/>).

## 1. Introduction

Membrane technologies are becoming more and more interesting due to lower energy consumption compared to other separation technologies [1,2]. Membrane technology, particularly reverse osmosis, can be used for potable water reuse [3] by removing even pathogens (bacteria and viruses) and low molecular mass chemical contaminants [4]. It is used in wastewater treatment [5,6] and in disease control [7]. Microfiltration is often used in pharmaceutical and other industries and is studied widely [8–12].

This paper focuses on contributing factors and their influence on the repeatability of the microfiltration process. Process repeatability is important from the process quality and safety aspects [13]. It is important to be able to estimate the number of cycles (time) the filter can withstand without damage or failure. Failure, in this case, is considered as filter clogging or penetration of bacteria, either by membrane damage or some kind of bacteria deformation [14]. The goal of the filter selection and validation is to ensure that the filter will operate without failure for the whole product batch [15]. The focus of this paper is on a small-scale laboratory experimental set, which was developed for laboratory testing since it is cheaper, faster, more controllable, and easier to change the process parameters [16,17]. It is beneficial to perform laboratory tests to select the proper filter and estimate its lifespan before actual filter implementation and process validation. Furthermore, some data may be acquired to be used in simulations or in advanced process control [18]. Repeatability

analysis and pressure measurements were made in a non-sterile environment, which makes them cheaper and less demanding for staff.

The goal of the testing was to find the worst-case process scenario and find the influential parameters that have an impact on the filter lifespan and the repeatability of the process. The worst-case scenario process parameters can then be used in the filter validation procedure.

The assumption was that the change in one parameter might have some effect on other parameters, and some data were collected that might be useful for the design process of new lines. The side effect of this analysis is the possibility of identifying a critical production process parameter (or parameters) and making some kind of parameter recording or control to increase the process reliability, process control, or possible failure detection [19].

Process repeatability is important for process stability and product quality. The results acquired during a stable and repeatable process are more reliable than a single set of data. Some statistical analysis must be used when comparing the process data on the laboratory and production lines. It is impossible to compare data when the process repeatability is poor. The poor repeatability of the first tests was the main reason for the analysis presented in this paper.

This filter system is used to keep the fluid level in a surge tank at a certain tolerance to enable consistent filling of the product in the final package. The mass tolerance in the final package can be as low as 0.001 g, so even the fluid level in the surge tank can have an influence on the stability of the filling process. It is easier to optimize the process (valve opening, pressure. . .) in case of a stable and repeatable process, which might lead to fewer valve operations and possible filter selection optimization.

The focus of this paper is on pressure oscillations taking place during system valve opening and closing and, consequently, the energy impact on the filter [20]. According to [20], the energy impact during valve opening is higher than during valve closing, so the article will focus on valve opening. In some cases, pressure oscillations can be used for fouling layer removal [21].

## 2. Materials and Methods

### 2.1. Filters

A wide spectrum of filter sizes were tested, from a single-layer filter to stacked filters. The membrane was hydrophilic Durapore polyvinylidene fluoride (PVDF) with 0.22  $\mu\text{m}$  pore size. The membrane area was between 3.5  $\text{cm}^2$  and 6900  $\text{cm}^2$ . The minimum size filter was a 3.9 cm long Optiscale 25 capsule with a 3.5  $\text{cm}^2$  filtration area with Luer Lok connections. This filter is referenced as small. The maximum size filter (large) tested was Opticap XL10 with a 6900  $\text{cm}^2$  filtration area, tri-clamp connections, and a cartridge length of 25 cm. The main limiting factor of filter size is tri-clamp fittings and filtering capacity at high filter pressure drop when pressure losses in hydraulic connections become significant due to increased fluid velocity.

### 2.2. Filtrate

For economic and possibly health issues, the laboratory experiments were limited to distilled water at approximately room temperature. The tests were made in a non-sterile environment at room temperature, and fluid was exposed to the environment. Some tests on small filters were made with substitutes. No significant discrepancies were observed, but due to the possible influence of substitute deterioration on process repeatability, the decision was made to present the results with distilled water.

### 2.3. Development of Experimental Lay-Out

The experimental layout consists of the hydraulic part and the measurement and control part. The testing procedure was developed, and nomenclature was defined to enable automatized data analysis.

### 2.3.1. Hydraulic Part

The experimental setup is shown in Figure 1. The siphon principle was applied, and pressurized nitrogen was used as the moving force.

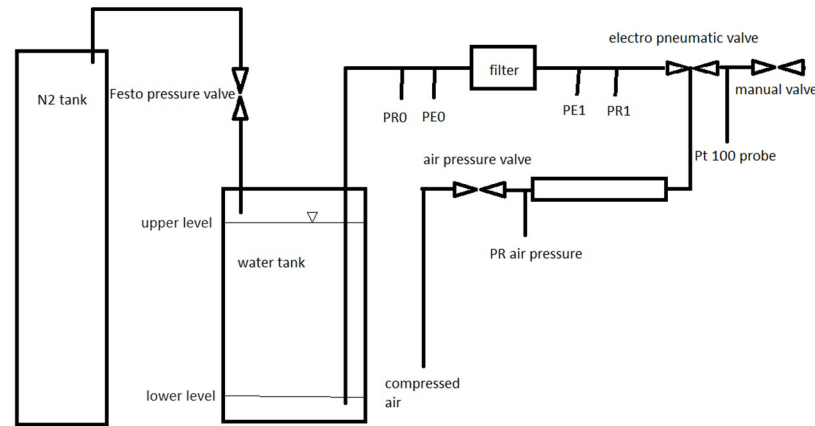


**Figure 1.** Scheme of the experiment.

The fluid supply part is the same as in [22], but the valve and pressure sensors were added. Gravity filtration [23] might be used for pressure drop approx. 0.1 bar [24]. Pump [25] was ruled out as one system was planned for all filters (3.5 cm<sup>2</sup> to 6900 cm<sup>2</sup> or even higher) and as pressure drop on the filter is a process parameter. (pressure drops 0.1, 0.3, 0.5, and 1 bar were set during testing). An 80-L water tank was used as the liquid supply. A Festo pressure regulator VPPM-6L-1-G18-0L2N-V1P-S1 (Festo SE & Co. KG, Esslingen am Neckar, Germany) was used for nitrogen pressure control. (Maximum hysteresis 10 mbar,  $\pm 0.5$  linearity, and repetition accuracy). The pressure was set by voltage signal (0–10 V, corresponding to 0–2 bar). The sensors, filter, and valve were connected by tri-clamp fittings. Two Keller PR-35X (KELLER Druckmesstechnik AG, Winterthur, Switzerland) piezoresistive sensors (PR0 and PR1) were used for static pressure measurements. The measurement range for PR0 was 3 bar, and the range for PR1 was 2 bar. Kistler 601 CAA (Kistler Holding AG, Winterthur, Switzerland) piezoelectric sensors with Kistler 5015 amplifiers were used for the pressure oscillation measurements (PE0 and PE1). Different filters with different fittings were analyzed; thus, some clamp adaptors were necessary. An electro-pneumatic valve, Burkert 2000 (Christian Bürkert GmbH & Co. KG, Ingelfingen, Germany), with an electric valve 6014 and tri-clamp connection, was controlled by a 24 VDC signal. According to [26], it was oriented 2→1 (movement of the plunger during valve opening in the same direction as fluid). An inductive sensor, RDP DCTH400AG (RDP Electronics Ltd., Wolverhampton, UK), was connected to the plunger to measure the valve lift. This parameter was used for the determination of valve opening/closing time and for an explanation of pressure diagrams [27]. The electro-pneumatic valve was driven by the compressed air, the pressure of which was controlled by a Fluidtec PR 4000 04 (FLUIDTEC AG, Kreuzlingen, Switzerland) pressure regulator. The compressed air pressure was measured by a Kistler piezoresistive sensor. Kern EOC 100K-3 (KERN & SOHN GmbH, Balingen, Germany) and Kern PCB 3500-2 (KERN & SOHN GmbH, Balingen, Germany) scales were used for the mass flow measurements. Filtered fluid was weighted in an open container to eliminate possible back-pressure issues, but some kind of fluid contamination is possible. In all cases, the pressures PE0 and PE1 were levelized by taking the corresponding PR (static) pressure and adding the PE (dynamic pressure) value.

### 2.3.2. Measurement and Control

A NI cRIO 9047 system was used for control and data acquisition. The modules NI 9215 (4 channel voltage analog input (0–10 V), NI 9203 (8 channel current analog input (0–20 mA), NI 9870 (4 channel RS-232 communication and a NI 9282/NI 9285 relay module

were used in NI cRIO. An analog output module NI 9269 integrated into a NI 9171 chassis was used for nitrogen pressure control. The LabVIEW, LabVIEW RT, and LabVIEW FPGA software were used. The nitrogen pressure control was controlled by the host PC. The main program was running on an FPGA. The program was built like a state machine, but there was no transition between the states. There were 3 states: manual, flow measurement, and pulse measurement.

Manual operation was used during setup and testing. During the flow measurement and dynamic measurements, all the pressures and plunger lift were measured simultaneously with a 50 kHz sampling frequency. The voltage inputs from the amplifiers and plunger lift signals were connected to a NI 9215 module. The Keller PR pressure sensors were connected to a 24 V power supply, and the analog current signal was connected to NI 9203. The Keller PR-35X sensors can be used with a K-114 amplifier (USB connection). In this case, the temperature compensation of measured values is possible, but the sampling frequency is limited to approx. 100 Hz. Additionally, it is practically impossible to synchronize USB sensors, AI signals, and DO (digital signals for valve control), so the decision was made to sacrifice temperature compensation and some accuracy for higher sampling frequency and synchronization. The sampling frequency of 50 kHz was a kind of trade-off to reduce the data quantity to reasonable levels. The resonant frequency of PE sensors exceeds 215 kHz [28], but the resonant frequencies of PR [29] and the inductive sensor [30] are much lower than 50 kHz. The system was designed and tested to acquire 6 channels for more than 10 s.

NI cRIO 9047 [31] has an 80 MHz internal base clock, so its influence of timing and synchronization delays on the process parameters will be neglected.

### 2.3.3. Testing Procedure

During all tests, the following procedure was followed:

Filling the tank with the fluid.

Removal of the gas in the fluid (system venting).

Setting the pressure level in the water tank to achieve the desired pressure drop on the filter.

Measurement of the fluid flow at the desired pressure drop.

Dynamic testing of 30+ repetitions.

Measurement of the fluid flow at the desired pressure drop.

The measurement of the fluid flow was repeated to control possible changes in the filter characteristics due to fouling [32]. The fouling might have been caused by some algae [33] or micro-corrosion in the water tank. Fouling was noticeable in the case of the small filters, especially since a significant amount of fluid had to be filtered during the filling of the system and system venting.

Dynamic tests were carried out under flow and no-flow conditions simply by switching the manual valve at the system exit to an open or closed position. The dynamic testing procedure was as follows: 0.5 s after the data recording started, the relay received the command to switch. The 24 VDC was switched to valve 6014, which delivered compressed air to the valve plunger and initiated the opening of the plunger. The fluid flow started. After the selected time (2 s to 6 s), valve 6014 was switched off, and the plunger closed the valve. It was also possible to carry out no-flow measurements by closing the manual valve at the system outflow and observing only plunger-induced pressure oscillations. Pressures were measured before and after the filter. Some pressure oscillations occurred, but their frequency and duration were filter size and fluid property (pressure, density. . .) dependent. The valve-induced pressure oscillations were used for the degassing of small filters and repeatability analysis of the electro-mechanical part of the system. Since piezo-electric (PE) sensors have a much lower response time than piezo-resistive (PR) sensors, they were chosen as the reference during the repeatability study of the dynamic phenomena.

#### 2.4. Statistical Analysis

The standard deviation was calculated from at least 30 repetitions. More than 35 dynamic tests were acquired, and the first 2–4 were discarded to enable the system to stabilize and improve the consistency of the results. The data were arranged according to measurement system time. Two contributing factors affect the standard deviation. The first is the difference in the amplitude of the signal, and the second is the time shift of the signals, which will be addressed in detail in Section 3.3.2.

#### 2.5. Filter Flow Rate Measurement

It is important to know the actual mass flow of the fluid through different filters at different pressure drops. Some phenomena, like the water hammer effect, are dependent on fluid flow. The focus of this paper is on the pressure waves during valve opening, but during the closing of the valve plunger, the induced oscillations combined with the water hammer effect. Scales were used for flow measurement, similar to [34], and RS-232 communication was applied for the values' transfer. The issue that occurred is that the serial communication module NI-9870 cannot operate with FPGA. This communication can work on the real-time controller of NI-9047, but not at the same frequency as it was used for pressure signal acquisition. The suitable sampling frequency for flow measurements is 1–5 Hz, so some adjustments and averaging were made for the pressure signals (p0 and p1 represent PR0 and PR1 after averaging). The results for flow measurement are presented in Figures 2 and 3. The program was run in a flow measurement state. After some time, the valve was opened by a mouse click, and after the desired time or quantity, it was closed by a mouse click. The mass flow was calculated via linear approximation of the cumulative mass curve. Some samples in the beginning and at the end of the measurement were discarded to reduce the influence of the transient regime during closing and opening. The proper measuring procedure for that kind of application is described in [35], but since filters are fouling constantly and due to the limited fluid capacity of the water tank, some simplifications were necessary. It was assumed that they do not reduce the accuracy of the mass flow results beyond an acceptable level.

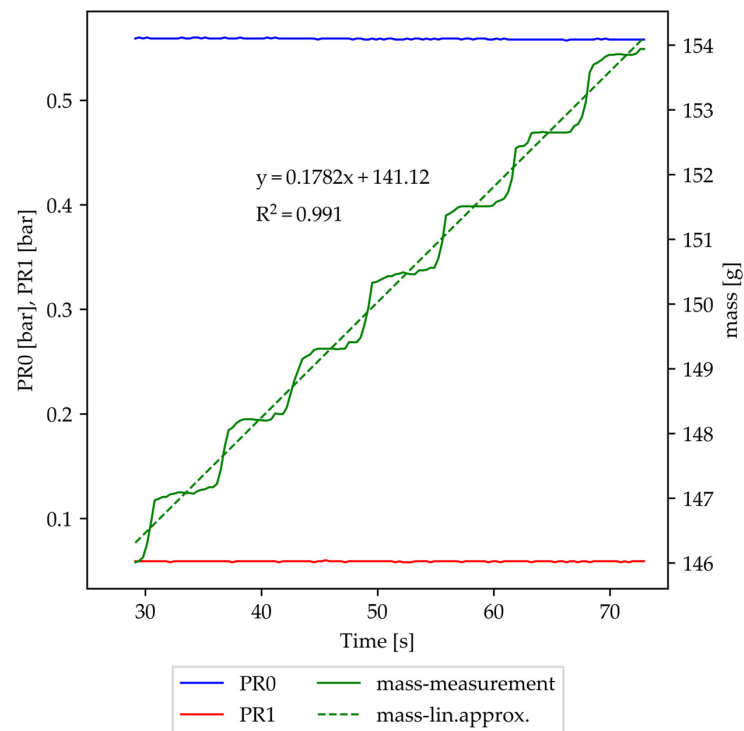


**Figure 2.** Flow measurement Optiscale 25 (pressure drop 0.5 bar) and linear approximation of the mass flow.

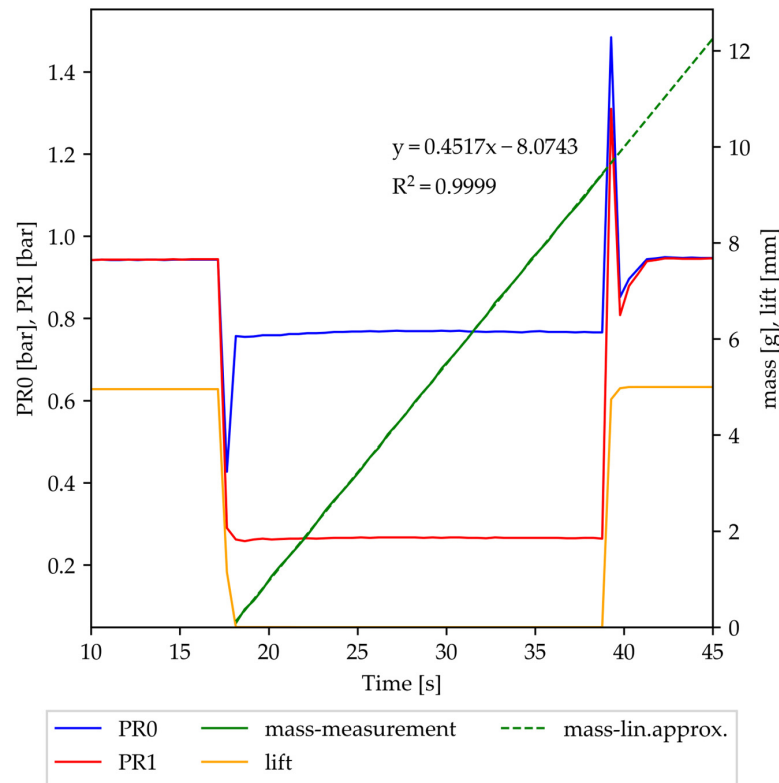


**Figure 3.** Flow measurement OpticapXL 10 (pressure drop 0.5 bar).

### 3. Results

#### 3.1. Flow Measurements

The minimum tubing inner diameter of 15.5 mm was too large for small filter mass flow measurements, but the decision was made to use the same connection elements as in a production line. The main difference is the usage of the smaller-scale Kern PCB with a 3.5 kg range and 0.01 g resolution. When filling the whole system with the fluid, it is possible to clog the small filter partially, and the low fluid velocity makes the degassing process complicated. Therefore, the probability increases of residual gas in the fluid and its effect on the repeatability of the results. Additionally, some flow oscillations may occur in the outlet tube. Figure 2 shows the mass flow measurement data and step-like curve of the total mass. Linear approximation can compensate for some of the error caused by over-dimensioned tubes in the case of low fluid flow in the case of small filters, low pressures, or both. As an additional control, some parameters were included in the file with dynamic measurement results. Those parameters included the timing of valve opening and closing and the current scale value. If some kind of fouling occurs during an extensive number of consecutive tests, it is possible to detect it by using the difference between the scale value and the actual time of the valve opening.

When measuring mass flow through large filters, the main problem is the high flow rate. It is hard to keep the pressure before the filter in the desired tolerance. It is possible to control the nitrogen pressure, but the change (decrease) of fluid level in the reservoir leads to a change in the total pressure before the filter, as shown in Figure 3. Please note that the static pressures PR0 and PR1 had to be set to 0.95 bar to achieve a dynamic pressure drop on the filter at 0.5 bar. In this case, the water hammer effect can result in a significant pressure peak during valve closing, especially if the pressure losses between the fluid reservoir and test system are significant.

The fluid pressure level was set to achieve a 0.5 bar pressure drop on the filter. The mass flow was 0.178 g/s (Optiscale 25), as shown in Figure 2, and 452 g/s (Opticap XL10) as shown in Figure 3.

### 3.2. Acquisition of Dynamic Data

Pressure diagrams acquired during dynamic testing were used to identify parameters influencing process repeatability and for filter energy intake calculation. Total acquisition time was between 5 s and 8 s, depending on the time required for fluid oscillations to disappear.

The dynamic test results (flow condition) for the large filter (opening and closing of the valve) are presented in Figure 4.

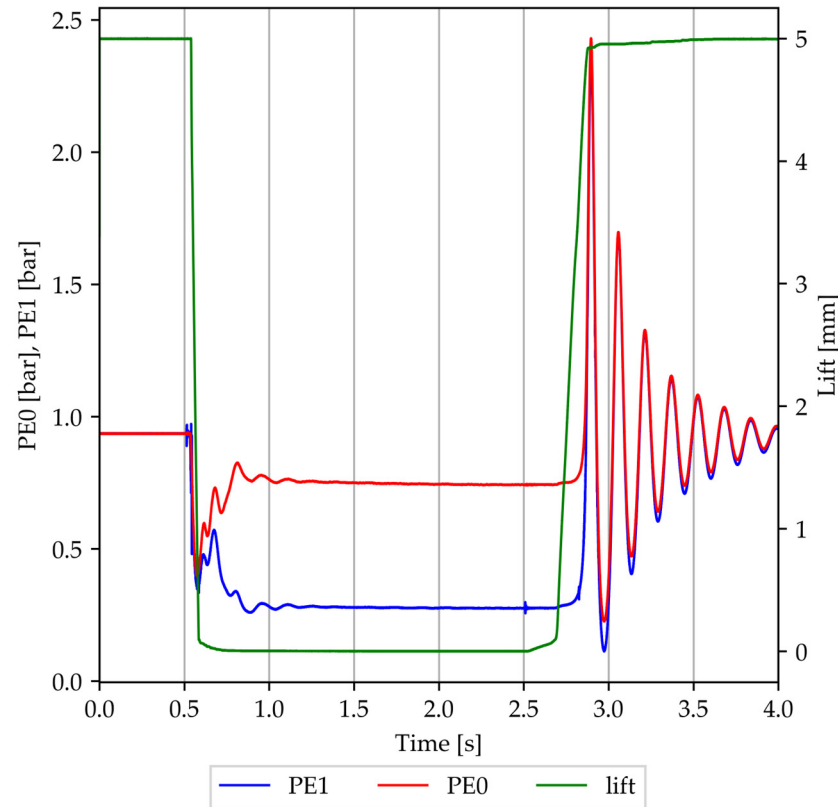


**Figure 4.** Pressure ahead and behind the filter (PE0 and PE1, respectively) and solenoid valve lift variation versus time acquired during large filter laboratory filter dynamic test—flow conditions.

As can be observed in Figure 4, there are some oscillations in both pressure curves. Almost 1 s is needed for pressure stabilization after valve opening. Pressures PE0 and PE1 are in phase and almost the same in amplitude during valve closing, contributing less to the filter energy intake [20]. There are some additional oscillations in the PE1 curve caused by plunger movements. PE0 and PE1 were placed before and after the filter, and the filter acted as a dampener, removing some of the high-frequency pressure oscillations in the PE0 signal. Sensor PE1 was also closer to the electro-pneumatic valve, causing pressure fluctuations, so it is the best reference parameter. A pressure difference (drop) on the filter can be observed as well. This is the main process parameter. The absolute pressure value is dependent on the cumulative pressure loss, which is highly dependent on the fluid mass flow. In this case, plunger movement lasted less than 0.05 s during valve opening and 0.15 s during closing.

The results for the small filter are presented in Figure 5. The time needed for pressure stabilization is shorter, and the frequency of oscillations is higher. The results can be used to define the valve opening process phase. The opening of the electro-pneumatic valve occurred at 0.515 s. Some valve-induced vibrations transmitted to the fluid and caused the pressure oscillations detected by the PE1 sensor. At 0.528 s, a change in the lift signal can be observed, indicating the separation of the plunger from the seat. At 0.535 s, a drop in the PE1 signal can be observed, indicating the start of the fluid flow.

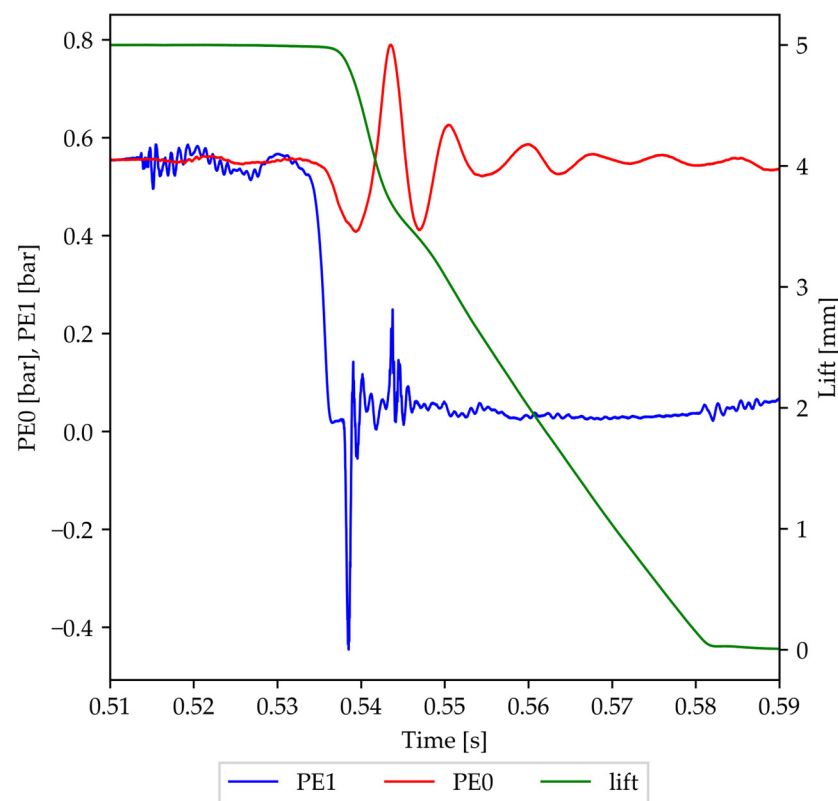


**Figure 5.** Pressure ahead and behind the filter (PE0 and PE1, respectively) and solenoid valve lift variation versus time acquired during valve opening with small laboratory filter (Optiscale 25) dynamic test—flow conditions.

### 3.3. Identification of Influential Parameters

Influential parameters can be divided into two groups. The first group consists of parameters that impact mostly on the pressure level. The parameters influencing process repeatability are placed in the second group. There is another parameter which will not be considered in this paper. This parameter is the internal diameter of the pipes and other elements in the setup. The internal diameter of all elements was at least 15.5 mm, but the length, shape, and arrangements of some connecting elements may vary, depending on the filter size and connector.

#### 3.3.1. Parameters Influencing the Pressure Level

##### Filter Size/Volume

Averaged pressure diagrams during valve opening for the large and the small filters are presented in Figure 6. The manual valve at the system outflow side (see Figure 1) was closed to avoid a flow-influenced phenomenon, like a water hammer effect.

As can be seen in the averaged pressure and its standard deviation curve presented in Figure 6, the duration of the pressure oscillations was much shorter and more intense in the case of the small filter, so for the rest of the paper, the focus will be on the small filter, which specific dynamic loads are higher. In this case, the size of the large filter and its fluid volume acted as a dumping factor, reducing the pressure peaks, standard deviation of the pressure signals, and repeatability of the plunger-induced pressure oscillations. The main process parameter was the filter pressure drop, i.e., the pressure difference before and after the filter during stable flow. Due to much higher-pressure losses, in-line and local losses within the system at high flow rates, the pressure level in the N<sub>2</sub> tank in the case of a big filter needs to be approx. 0.4 bar higher than in the case of a small filter to achieve the same filter pressure drop, as can be seen in Figure 7.

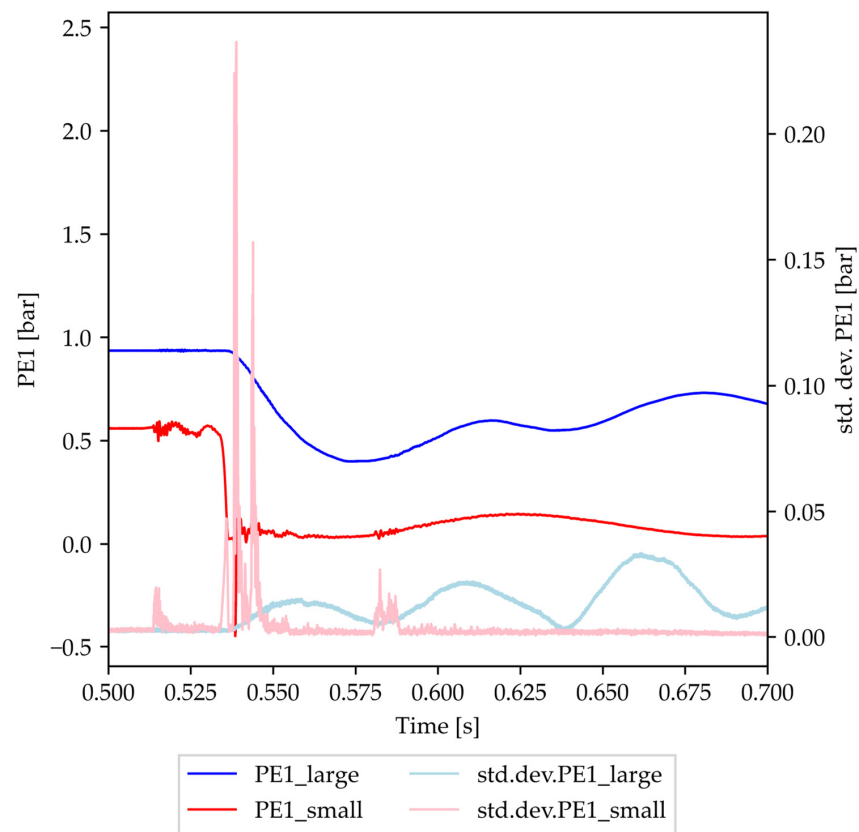


**Figure 6.** Pressure behind the filter (PE1) and standard deviation versus time acquired during valve opening with large (Opticap XL10) and small filter (Optiscale 25) dynamic test—no-flow conditions.

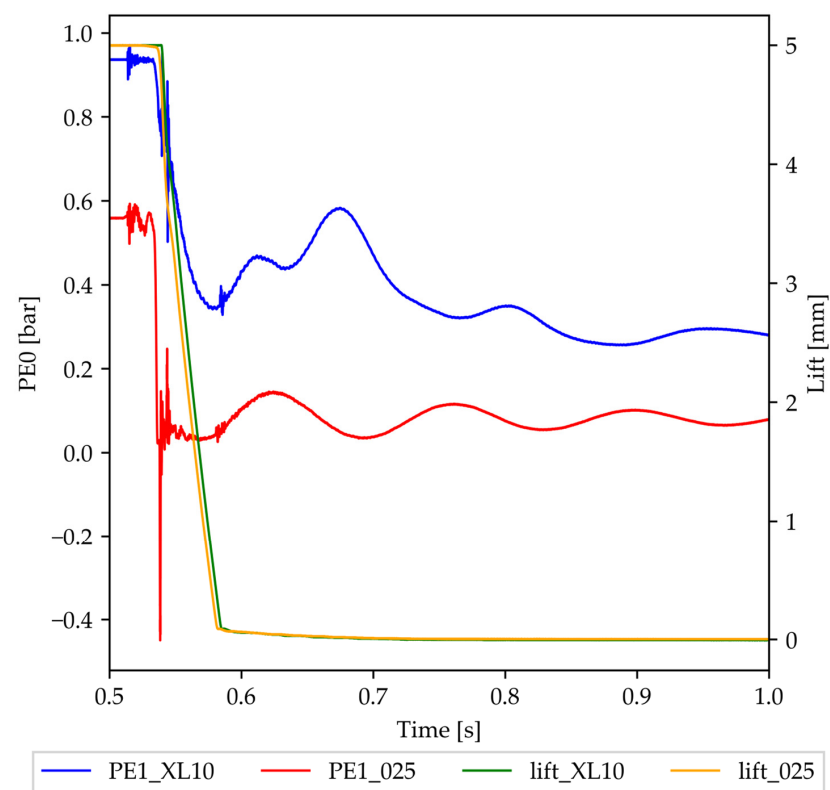


**Figure 7.** Pressure behind the filter (PE1) and plunger lift versus time acquired during valve opening with large (Opticap XL10) and small filter (Optiscale 25) dynamic test—flow conditions.

Figure 7 shows the difference between the small and large filters under fluid flow conditions (manual valve open). The pressure gradient was higher in the case of the small filter. It is also interesting to observe the movement of the plunger (lift). The movement of the plunger in the case of the smaller filter started 2 ms sooner, while the change in the lift gradient occurred a little later. The main reason for this was the higher fluid pressure and lower cumulative force on the plunger in the case of the large filter. The standard deviation of the pressure was higher in the case of the smaller filter, so this is another validation of the hypothesis that the smaller filter is more interesting when repeatability is an issue. It is possible to observe pressure oscillations at 0.580 s (Optiscale 25) and 0.582 s (Opticap XL10). Those oscillations occur when the plunger hits the seat at its final position.

### Fluid Pressure

As stated, the main process parameter (as on the production line) was the pressure drop on the filter, and since system pressure losses depend highly on fluid flow rate, different pressures within the water tank (see Figure 1) and thus within the whole system were applied for different filters. A higher pressure in the system can have a significant effect on the fluid properties, especially when the residues of gas are present. The existence of some minor gas bubbles in the filter or near the seals could not be ruled out, and absolute pressure can have a significant effect on the size and compressibility module of the fluid and, consequently, the velocity of sound and the resonant frequency. In order to analyze the influence of water tank pressure level on repeatability, the tests (30 repetitions) were performed with a 0.1, 0.3, 0.5, and 1 bar pressure drop on the small size filter (Optiscale 25) and averaged pressure traces and corresponding standard deviation curves are presented in Figure 8. The pressure drop on the filter might be considered transmembrane pressure, but since pressure sensors are placed in a T-type fitting and there are some additional pressure losses in sealings, filter housing, and reduction fittings, the exact transmembrane pressure is a little lower than the pressure drop.

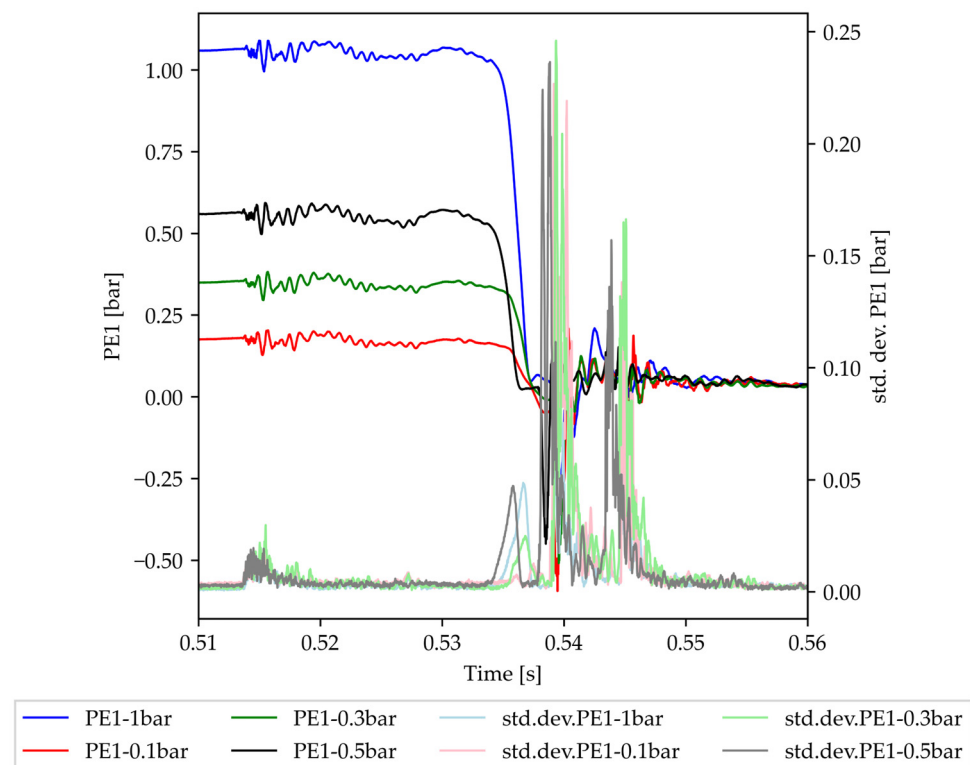


**Figure 8.** Averaged pressure traces behind the filter (PE1) and standard deviation curves acquired during valve opening with medium size filter (Opticap 25); dynamic test—flow conditions filter pressure drop 1.0 bar, 0.5 bar, 0.3 bar, and 0.1 bar, respectively.

The results presented in Figure 8 show that the pressure oscillations started at the same time in all four cases, but the shifted pressure peaks and different pressure amplitudes pointed to a possible change in the fluid's compression module due to different amounts of dissolved small gas bubbles. Generally, a higher gas content reduces the pressure peaks. It is possible to observe differences in the pressure gradient in the time interval between 0.535 s and 0.540 s (see Figure 9). This is another effect of the increased water tank pressure. It increases plunger speed during valve opening by increasing cumulative force acting on the plunger. As a result, the pressure drop gradient increases with water tank pressure, which can be observed in Figure 9. By focusing on the interval when the plunger starts to move, as presented in Figures 9 and 10 and defined in Figure 11, it can be observed that the standard deviation values were almost the same regardless of the static pressure but sometimes shifted too, as more time is required to accumulate adequate pressure. The main peaks in the standard deviation correspond to the maximum changes in the pressure diagram, like the starting or stopping of the plunger movement. The plunger movement depends on cumulative force, and all forces except the fluid compression force were the same. The time required for the compressed air force in the valve to overcome other forces is dependent mostly on fluid pressure. The lowest standard deviation values can be observed in the case of the 1 bar filter pressure drop (1.06 bar static pressure). Most likely, the residual gas was dissolved in the fluid, increasing its homogeneity. An additional explanation can be that pressure forces are usually more predictable than friction forces. According to the authors' experience, at least the first two tests varied significantly from the others. Sometimes, even the next two were somewhat different (usually after a prolonged stop in the measurements). That is why 35+ repetitions were acquired, and the first four were not considered in the statistical analysis.

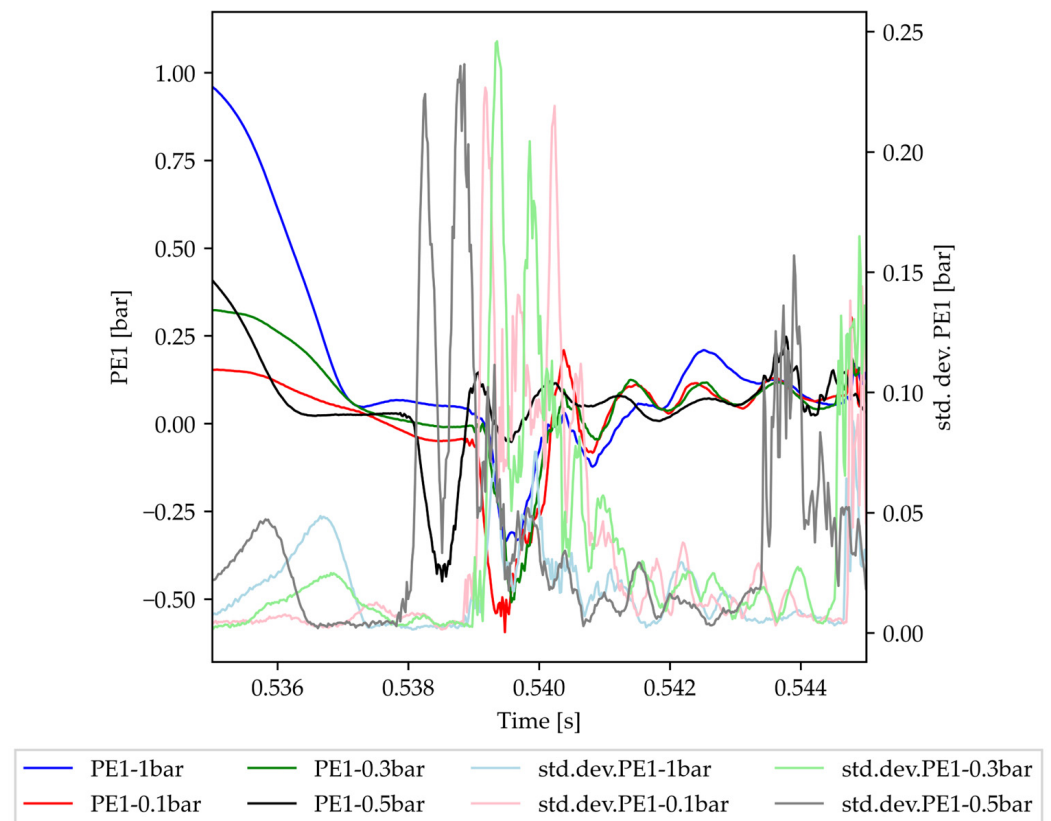


**Figure 9.** Close-up of Figure 8. Focus is on the beginning of the plunger movement.

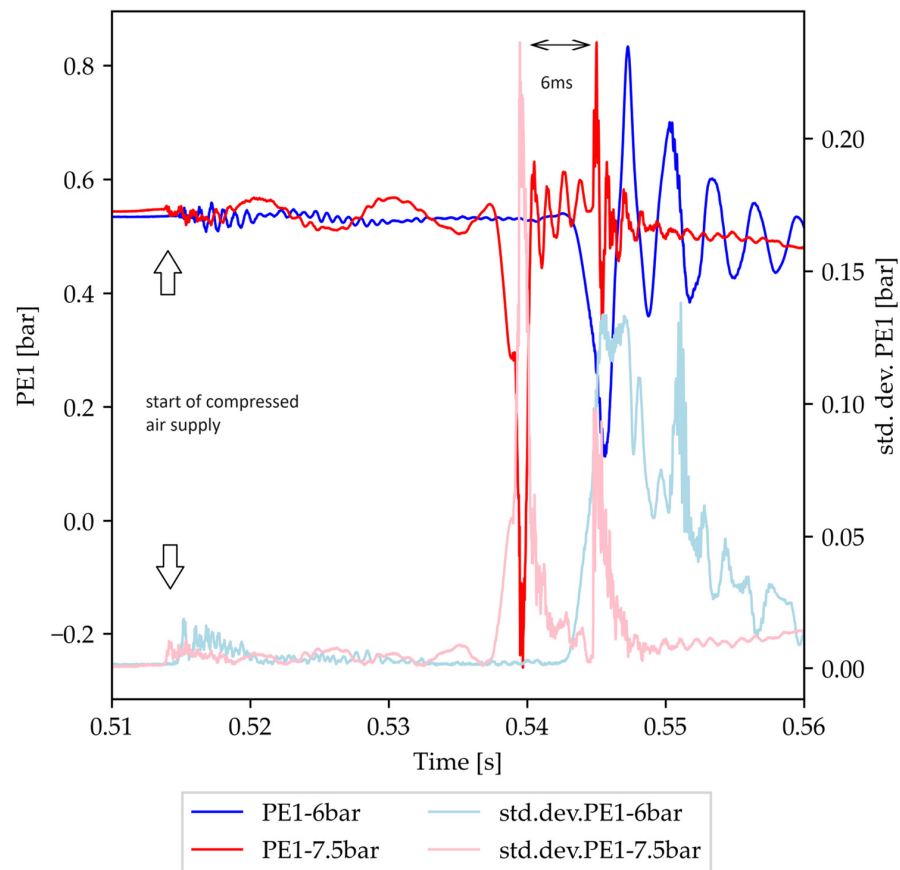


**Figure 10.** Averaged pressure behind the filter (PE1) and corresponding standard deviation versus time acquired during valve opening with 7.5 bar and 6.0 bar compressed air pressure; small filter (Optiscale 25) dynamic test—no-flow conditions.

#### Valve Plunger Speed

The electro-pneumatic valve plunger speed is dependent mostly on the compressed air pressure, but, as presented in Figure 8, the fluid pressure has some impact as well, associated mostly with the starting of the plunger movement (the first valley in the corresponding pressure diagram). The tests shown in this chapter were made with a small filter and a 0.5 bar pressure drop. The pressure regulator and pressure chamber were used to minimize the influence of the compressed air pressure oscillations. Two pressure levels were tested, and two lengths of the tube between the pressure chamber and the valve were tested to simulate some parameters that can happen during production.

The goal of the experiment was to test the extreme values, so the measurements were performed at 7.5 bar and 6 bar. The pressure level tolerance was 0.02 bar. According to the documentation [30], the minimum operating pressure for the electro-pneumatic valve is 4 bar. The influence of compressed air tube length will be discussed in Section 3.3.2. The average value and standard deviation of the signals are presented in Figure 10. The manual valve at the end was closed (no-flow conditions) to eliminate the fluid flow and fluid properties related to contributing factors. When there is no flow, the gas bubbles that might be trapped in the fluid cannot escape, and the fluid temperature is constant. Thus, the testing conditions do not vary a lot.

As can be observed in Figure 10, the compressed air supply started at almost the same time (0.514 s), as shown on the pressure and standard deviation curve. The minimum PE1 pressure level occurred with approx. 7 ms delay and at 0.2 bar lower amplitude in the case when 6 bar compressed air was used. The influence of the compressed air pressure on the plunger lift is presented in Figure 11. The movement of the plunger was delayed by

approximately 6 ms, and the final position was reached approximately 17 ms later when the pressure was 6 bar.

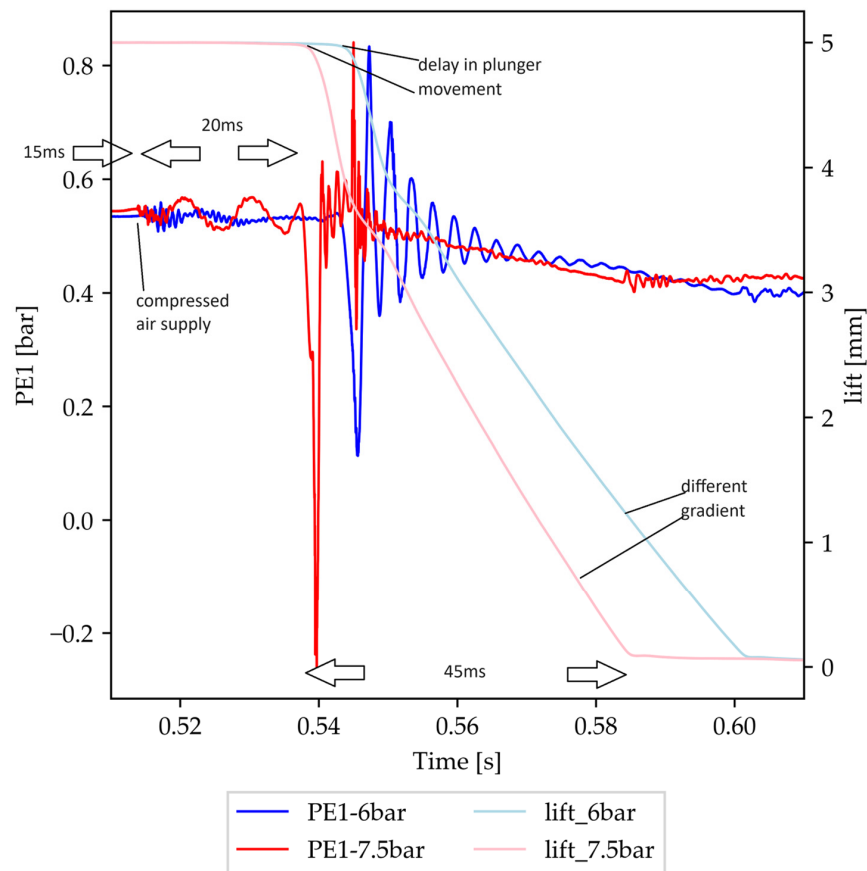


**Figure 11.** Averaged pressure behind the filter (PE1) and plunger lift versus time acquired during valve opening with 7.5 bar and 6.0 bar compressed air pressure; small filter (Optiscale 25) dynamic test—no-flow conditions.

There was a change in the lift gradient of approximately 5 ms after the start of the movement. It is assumed that this corresponded to the change in the internal geometry of the valve. The plunger (valve orientation 2→1 was applied) moved mostly in the general flow direction, resulting in a negative pressure gradient at the beginning of the movement and a positive pressure gradient when the valve was at least partially open. It is possible to estimate the time required for specific phases during valve opening (values for 7.5 bar air pressure): 15 ms between the command and starting of the compressed air supply, 20 ms starting of the plunger movement, and 45 ms until the plunger stops.

So far, process parameters have been discussed; however, the applied hardware may also influence process repeatability.

### 3.3.2. Parameters Influencing Process Repeatability

#### Timing/Relay

There are two relays available for a cRIO system. NI 9482 is a 4-channel electro-mechanical relay, and NI 9485 is an 8-channel semiconductor relay. NI 9482 is suitable for higher switching currents, and that is why it was used in the first system. The compressed air pressure and fluid pressure were the same. The compressed air repeatability pressure interval was  $\pm 0.05$  bar, and the fluid pressure interval was  $\pm 0.02$  bar. It was observed that the first 3–5 cycles had a higher spread due to the different frictions of the plunger, so they were discarded, and only the last 30 are presented in Figure 12.

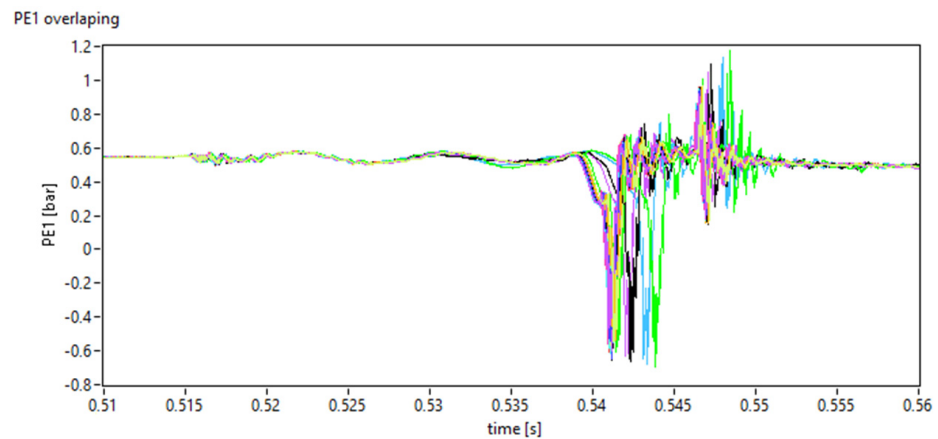


**Figure 12.** Overlapping of the PE1 signals acquired during valve opening with the application of semiconductor relay NI-9482; small filter (Optiscale 25) dynamic test—no-flow conditions.

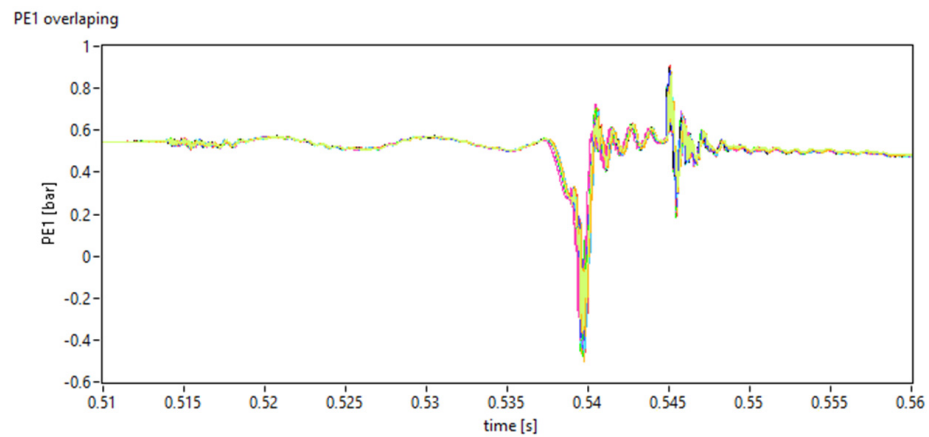


**Figure 13.** Overlapping of the PE1 signals acquired during valve opening with the application of semiconductor relay NI-9485; small filter (Optiscale 25) dynamic test—no-flow conditions.

As can be observed in Figure 12, the first disturbance of the pressure signal can be observed 15 ms after the switch. This corresponds to the starting of the compressed air supply via activation of the electric valve. The peak values between 0.54 s and 0.545 s correspond to the plunger movement. It is possible to observe the time spread of approximately 3 ms. The procedure was repeated with the semi-conductor relay NI-9485. The results are presented in Figure 13.

By comparison of Figures 12 and 13, it is possible to observe that NI-9485 was a little faster (approx. 1 ms), but the repeatability was much better in this case. There was not much difference between the spread close to the electro-pneumatic valve opening in Figures 12 and 13, but it is obvious when the pressure amplitudes were higher, pointing to the importance of the parameters in the initial phase of the valve opening/start of air supply [36]. There is a correlation between the spread and the relay bounce time (3 ms), as defined in [37]. The spread in time can influence the average value like a high-pass filter. The mean value and standard deviation of the signals are presented in Figure 14. The time delay of approx. 1 ms can be observed again, and the slight difference in the amplitude of the averaged signal can be seen as well. The peak of standard deviation was higher and wider when NI 9482 was used, pointing to worse repeatability.

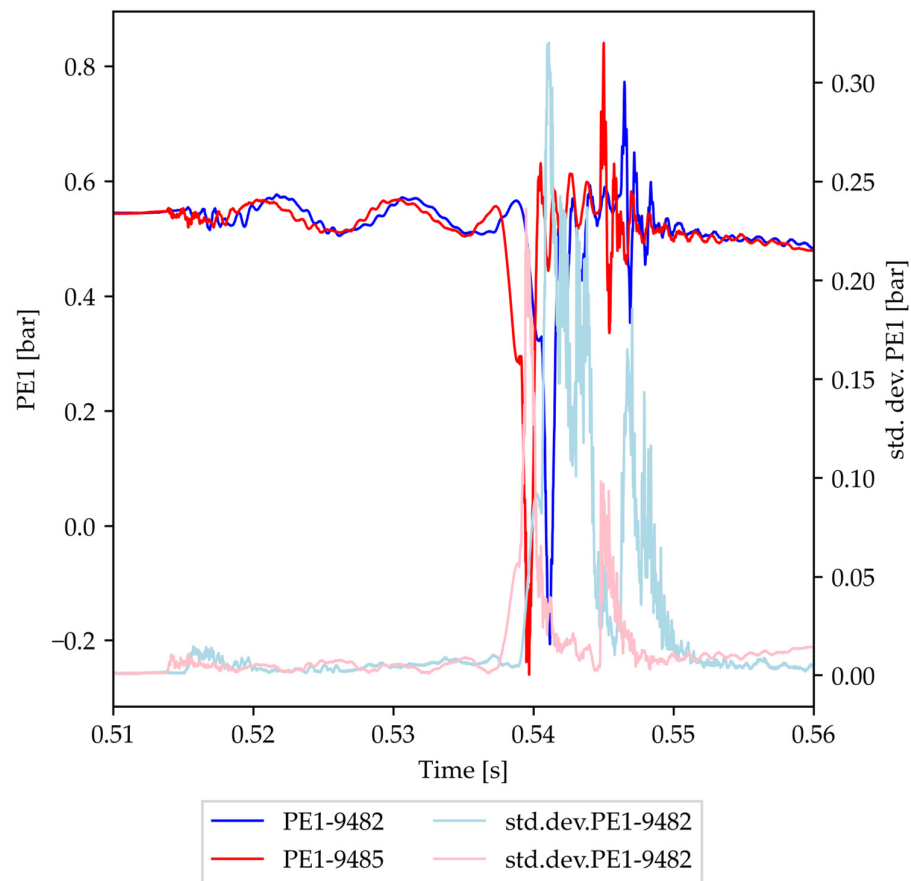


**Figure 14.** Comparison of averaged PE1 signals and corresponding standard deviation acquired during valve opening with application of relays NI-9482 and NI-9485; small filter (Optiscale 25) dynamic test—no-flow conditions.

#### Valve Opening Speed

The movement of the plunger is controlled by four forces. Compressed air is used for opening, and a spring is used for closing. Friction forces and fluid pressure forces occur as well. The last two are mostly constant after three to five cycles. The pressure difference on the filter was set to 0.5 bar. The most influential parameter was compressed air pressure and its drop after the valve opening. An approximately 1 dm<sup>3</sup> volume pressure reservoir was used for pressure stabilization. The influence of the compressed air pressure level was addressed partially in Figure 10. The peak of the standard deviation of the PE1 signal was concentrated close to the extreme pressure level in the case of 7.5 bar. The peak of the standard deviation in the case of 6 bar was wider, which hints at a wider spread of the results. Since approx. 4 bar pressure is needed to overcome spring force, higher pressure results in a faster and more consistent plunger movement.

Two compressed air tube lengths were used to study the influence of tube length on process stability. Both tubes were plastic with an internal diameter of 8 mm. The Short Tube (ST) was 200 mm long, and the Long Tube (LT) was 20 m long. The results are presented in Figure 15.

The results presented in Figure 15 show the significant effect of the tube length on the averaged pressure curve. The averaged PE1 pressure valley value was smaller in the case of the longer tube. Together with the wider spread of standard deviation, it leads to the conclusion of worse repeatability. Please note that the peak of the standard deviation of PE1 in the case of the shorter tube was located close to the valley pressure value, while it was shifted in the case of the longer tube.

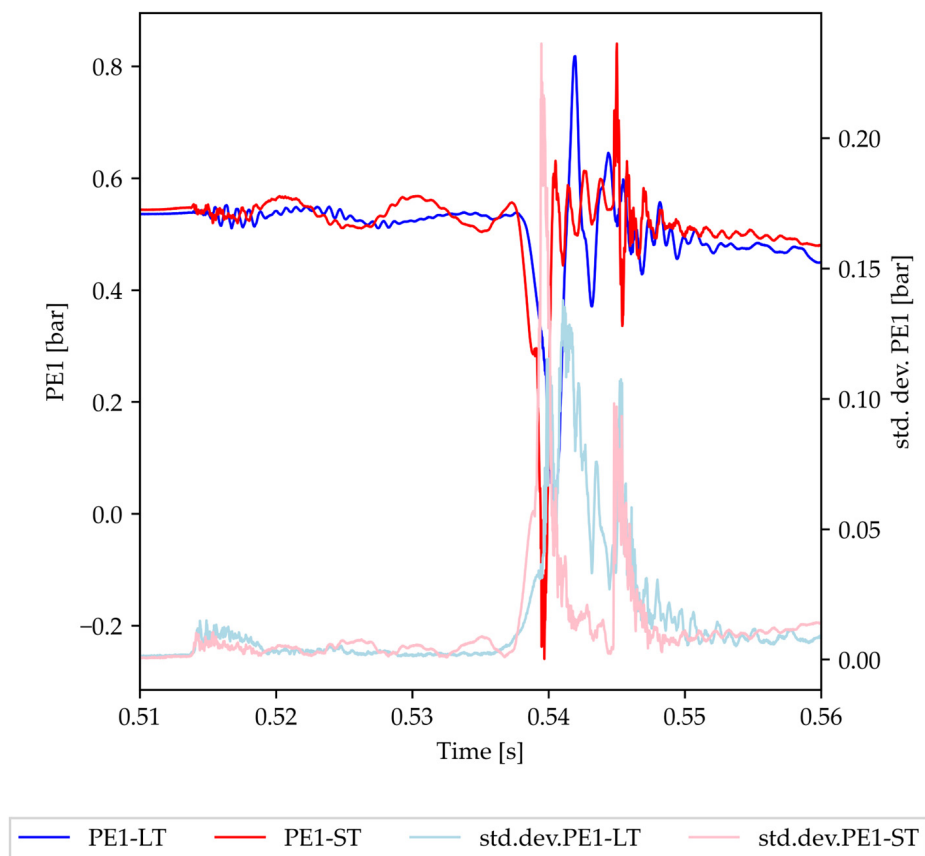


**Figure 15.** Comparison of averaged PE1 signals and corresponding standard deviation acquired during valve opening with application of long (LT) and short (ST) compressed air tube; small filter (Optiscale 25) dynamic test—no-flow conditions.

#### 4. Discussion

The presented system was used for flow measurements and dynamic tests. The main purpose of acquired dynamic data was the calculation of the stress acting on the filter [20]. The results are presented in Table 1. It can be observed that the filter energy intake increased with the compressed air pressure. The longer tube resulted in lower energy intake but resulted in worse repeatability. A practical industrial solution might be the introduction of a pressure reservoir in conjunction with the pressure regulator close to the valve. The statistical analysis of the measured data increased the confidence in the energy intake calculation.

**Table 1.** Comparison of filter energy intake.

Tube Length	Compressed Air Pressure	Fluid Pressure Drop on the Filter	Energy Intake (Opening)
200 mm	6 bar	0.5 bar	1.5 J/m <sup>2</sup>
200 mm	7.5 bar	0.5 bar	2.1 J/m <sup>2</sup>
20 m	7.5 bar	0.5 bar	1.75 J/m <sup>2</sup>

The system enables measurement of mass flow for different filters and the closing and opening times of the valve. When those parameters are known, it is possible to optimize the surge tank filling procedure and reduce the number of valve cycles. In this case, the actual relay characteristics must be measured to know the time delay and possible bouncing period, maybe even considering them during the designing process.

It is possible to adjust the system to smaller filters and smaller fluid flows by replacing the outlet tube with a smaller diameter tube. Modifications that can improve the repeatability

bility in the case of larger fluid flow are associated mostly with the flow intake. The focus should be on reducing the pressure losses before the filter and a larger fluid reservoir with a larger diameter to reduce the effect of the fluid level. The other possibility is an adaptive control of the nitrogen pressure to compensate for the drop in the fluid level.

The influence of compressed air pressure was studied, and possible improvements were suggested. Furthermore, it was possible to measure and observe dependencies between the influential parameters, which might be useful during possible process simulation or digital twin setup.

## 5. Conclusions

A laboratory scale filtering system was implemented successfully and used for measurements with filters of various sizes. It was equipped with several sensors to enable better insight into the filtering process, pressure oscillations, and stresses on the filter. It is possible to test different filters if they have compatible tri-clamp connections. The system had a high level of automation but still enabled the operator to choose the opening and closing times of the valve and total recording time to focus on the desired phase of the process. It is also possible to automate the measuring procedure to run for a desired number of cycles and collect data connected to filter fouling or failure.

The process parameters with the highest impact on process repeatability were identified, and the repeatability of the laboratory layout was improved. Some possible solutions to improve production line repeatability were suggested.

Possible further improvement might be the usage of the signals for mass flow determination [38] and possibly in situ non-intrusive filter fouling estimation.

**Author Contributions:** G.B.: Conceptualization, Software, Writing—original draft; L.K. Investigation; G.H. Formal analysis; D.K., Resources, Supervision; A.K., Resources; J.R. Formal analysis, Methodology; M.H., Supervision; A.H. Conceptualization, Methodology. All authors have read and agreed to the published version of the manuscript.

**Funding:** This research was funded by the Slovenian Research Agency (Research core funding No. P2-0196) and Novartis Pharma.

**Data Availability Statement:** Data are contained within the article.

**Conflicts of Interest:** Authors Grega Hrovat, Drago Kuzman and Aleks Kapun were employed by the company Novartis Pharma. The remaining authors declare that the research was conducted in the absence of any commercial or financial relationships that could be construed as a potential conflict of interest. The authors declare that this study received funding from Novartis Pharma. The funder was not involved in the study design, collection, analysis, interpretation of data, the writing of this article or the decision to submit it for publication.

## References

1. Drioli, E.; Stankiewicz, A.I.; Macedonio, F. Membrane engineering in process intensification—An overview. *J. Membr. Sci.* **2011**, *380*, 1–8. [[CrossRef](#)]
2. Anis, S.F.; Hashaikeh, R.; Hilal, N. Microfiltration membrane processes: A review of research trends over the past decade. *J. Water Process. Eng.* **2019**, *32*, 100941. [[CrossRef](#)]
3. Tang, C.Y.; Yang, Z.; Guo, H.; Wen, J.J.; Nghiem, L.D.; Cornelissen, E. Potable Water Reuse through Advanced Membrane Technology. *Environ. Sci. Technol.* **2018**, *52*, 10215–10223. [[CrossRef](#)] [[PubMed](#)]
4. Council, N.R. *Water Reuse: Potential for Expanding the Nation's Water Supply through Reuse of Municipal Wastewater*; National Academies Press: Washington, DC, USA, 2012.
5. Pizzichetti, A.R.P.; Pablos, C.; Álvarez-Fernández, C.; Reynolds, K.; Stanley, S.; Marugán, J. Kinetic and mechanistic analysis of membrane fouling in microplastics removal from water by dead-end microfiltration. *J. Environ. Chem. Eng.* **2023**, *11*, 109338. [[CrossRef](#)]
6. Al-Tayawi, A.N.; Sisay, E.J.; Beszédes, S.; Kertész, S. Wastewater Treatment in the Dairy Industry from Classical Treatment to Promising Technologies: An Overview. *Processes* **2023**, *11*, 2133. [[CrossRef](#)]
7. Košir, T.; Fric, K.; Filipić, A.; Kogovšek, P. Bacterial Filtration Efficiency of Different Masks. *Stroj. Vestn.-J. Mech. Eng.* **2022**, *68*, 225–232. [[CrossRef](#)]



36. Lisowski, E.; Filo, G.; Rajda, J. Analysis of Flow forces in the initial phase of throttle gap opening in a proportional control valve. *Flow Meas. Instrum.* **2018**, *59*, 157–167. [[CrossRef](#)]
37. NI. User Manual and Specifications NI 9482. Available online: <https://www.ni.com/docs/de-DE/bundle/ni-9482-specs/resource/373948b.pdf> (accessed on 15 September 2023).
38. Zhang, J.; Wang, D.; Xu, B.; Su, Q.; Lu, Z.; Wang, W. Flow control of a proportional directional valve without the flow meter. *Flow Meas. Instrum.* **2019**, *67*, 131–141. [[CrossRef](#)]

**Disclaimer/Publisher’s Note:** The statements, opinions and data contained in all publications are solely those of the individual author(s) and contributor(s) and not of MDPI and/or the editor(s). MDPI and/or the editor(s) disclaim responsibility for any injury to people or property resulting from any ideas, methods, instructions or products referred to in the content.